

# Prevalence of Subclinical CNV and Choriocapillaris Nonperfusion in Fellow Eyes of Unilateral Exudative AMD on OCT Angiography

Alison D. Treister<sup>1</sup>, Peter L. Nesper<sup>1</sup>, Alaa E. Fayed<sup>1,2</sup>, Manjot K. Gill<sup>1</sup>, Rukhsana G. Mirza<sup>1</sup>, and Amani A. Fawzi<sup>1</sup>

<sup>1</sup> Department of Ophthalmology, Feinberg School of Medicine, Northwestern University, Chicago, IL, USA

<sup>2</sup> Department of Ophthalmology, Kasr Al-Ainy School of Medicine, Cairo University, Cairo, Egypt

**Correspondence:** Amani A. Fawzi, Department of Ophthalmology, Feinberg School of Medicine, Northwestern University, 645 N. Michigan Avenue, Suite 440, Chicago, IL 60611, USA. e-mail: afawzimd@gmail.com

**Received:** 1 April 2018

**Accepted:** 23 August 2018

**Published:** 1 October 2018

**Keywords:** age-related macular degeneration; choriocapillaris; choroidal neovascularization; OCT; optical coherence tomography angiography

**Citation:** Treister AD, Nesper PL, Fayed AE, Gill MK, Mirza RG, Fawzi AA. Prevalence of subclinical CNV and choriocapillaris nonperfusion in fellow eyes of unilateral exudative AMD on OCT angiography. *Trans Vis Sci Tech.* 2018;7(5):19, <https://doi.org/10.1167/tvst.7.5.19>  
Copyright 2018 The Authors

**Purpose:** To determine the prevalence of subclinical choroidal neovascularization (CNV) in fellow eyes of patients with unilateral exudative age-related macular degeneration (AMD) using optical coherence tomography angiography (OCTA) and to quantify choriocapillaris nonperfusion adjacent to CNV.

**Methods:** We retrospectively reviewed all patients with AMD who underwent OCTA and identified eyes with unilateral exudative AMD. We determined the presence of subclinical CNV on custom en face macular slabs of the outer retina and choriocapillaris and confirmed on cross-sectional scans. Two graders quantified the percent choriocapillaris area of nonperfusion (PCAN) in the entire choriocapillaris slab as well as in the “halo” zone (200  $\mu$ m) surrounding subclinical and exudative CNV lesions.

**Results:** Of 140 AMD patients who underwent OCTA, 34 had unilateral exudative AMD, with five of the 34 fellow eyes (14.7%) having subclinical CNV. Compared with PCAN in the entire slab ( $10.333 \pm 4.288\%$ ), we found that “halo” PCAN, surrounding CNV, was significantly higher ( $13.045 \pm 5.809\%$ ;  $P < 0.001$ ). Further, there was a trend for higher PCAN in exudative CNV eyes ( $15.267 \pm 7.230\%$ ) compared with their fellow subclinical CNV eyes ( $10.823 \pm 3.365\%$ ,  $P = 0.115$ ).

**Conclusions:** There is a notable prevalence of subclinical CNV in fellow eyes with unilateral exudative CNV, and significantly greater choriocapillaris nonperfusion adjacent to all CNV lesions. We identified a trend for increased choriocapillaris nonperfusion in exudative AMD eyes as compared with their fellow subclinical CNV eyes, which deserves further study.

**Translational Relevance:** OCTA can be useful in clinical practice to detect subclinical CNV and study choriocapillaris dysfunction.

## Introduction

Age-related macular degeneration (AMD) is a leading cause of blindness globally.<sup>1</sup> Patients with AMD can progress to an advanced stage of disease, including geographic atrophy or exudative AMD.<sup>2</sup> Exudative AMD is characterized by choroidal neovascularization (CNV), the growth of new blood vessels that lead to vision loss and distortion due to leakage into surrounding tissue.<sup>2</sup> In patients with unilateral exudative AMD, it is important to consider

the fellow eye as there is a 42% risk of CNV within 5 years.<sup>3</sup>

Subclinical CNV was first described in histologic specimens by Green et al.<sup>4</sup> and Sarks et al.<sup>5</sup> These researchers noted abnormal choroidal vessels passing through breaks in the Bruch's membrane in postmortem eyes that had no overlying hemorrhage or exudation.<sup>4,5</sup> At that time, it was hypothesized that these lesions predated exudation. Yannuzzi et al.<sup>6</sup> later showed that indocyanine-green angiography (ICGA) could be used to detect subclinical CNV

lesions as hyperfluorescence with late staining of choroidal vessels. ICGA was performed in conjunction with fluorescein angiography (FA); however, FA was shown to be limited by lack of penetration into the choroid as well as more leakage due to lower affinity for large proteins.<sup>6</sup> By studying 432 fellow eyes of patients with unilateral exudative AMD, Hanutsaha et al.<sup>7</sup> found an 11% prevalence of hyperfluorescent plaques on ICGA. These authors suggested that these plaques could predict exudation. Over a mean follow-up of 22 months, exudation occurred in 24% of eyes with plaques as compared with 11% of eyes without.<sup>7</sup> While studies have shown the utility of ICGA in assessing subclinical CNV and risk of exudation, the use of this imaging modality has been limited.

Optical coherence tomography angiography (OCTA) is an imaging technique that allows noninvasive visualization of retinal and choroidal blood flow in a variety of disorders, including AMD.<sup>8</sup> Compared with ICGA, the sensitivity and specificity of OCTA in detecting subclinical CNV was reported at 81.8% and 100%, respectively.<sup>9</sup> The prevalence of subclinical CNV in patients with unilateral exudative AMD has ranged from 6.25% to 27%.<sup>10–13</sup> It is important to estimate the prevalence subclinical CNV in these fellow eyes, as their risk of exudation is 15 times greater than fellow eyes without subclinical CNV.<sup>10</sup>

In addition to using OCTA to detect subclinical CNV, this approach can visualize choriocapillaris flow.<sup>14,15</sup> While choriocapillaris imaging suffers from light scattering from the overlying retinal pigment epithelium (RPE), the resultant bright pixels have been shown to represent flow and vary predictably with AMD.<sup>14,16,17</sup> There is increasing evidence for the role of choriocapillaris dysfunction in the pathogenesis of AMD and a need to further characterize choriocapillaris pathology in AMD.<sup>18–21</sup> We initiated this retrospective, cross-sectional study to (1) determine the prevalence of subclinical CNV in patients with unilateral exudative AMD at a tertiary care center, (2) quantitatively assess choriocapillaris flow in areas adjacent to CNV, and (3) quantitatively compare choriocapillaris flow in eyes with exudative AMD to their fellow eyes with subclinical CNV. We hypothesized that choriocapillaris nonperfusion would be more evident in the areas adjacent to CNV formation and that exudative AMD eyes would have more severely compromised choriocapillaris compared with their fellow subclinical CNV eye.

## Methods

In this retrospective, cross-sectional study, patients with exudative AMD were identified from a cohort of patients presenting between October 2016 and September 2017 to the Department of Ophthalmology at Northwestern University in Chicago, IL. Patients underwent imaging with OCTA and clinical examination by their respective retinal physician. This study was approved by the institutional review board of Northwestern University and followed the tenets of the Declaration of Helsinki. Informed consent was obtained from all patients after explanation of the nature and possible consequences of the study.

### Study Sample

Study subjects were obtained from a cohort of patients with a diagnosis of AMD treated by one of three retina specialists (AAF, MKG, and RGM) and with at least one prior OCTA scan. Inclusion in this study required a diagnosis of exudative AMD in one eye and nonexudative AMD in the fellow eye, irrespective of their AMD stage. Unilateral exudative AMD eyes had subretinal or intraretinal fluid at the time of OCTA imaging or a prior history of subretinal or intraretinal fluid requiring anti-vascular endothelial growth factor (anti-VEGF) therapy. Patients were excluded if they had prior treatment with anti-VEGF therapy or disciform scar in the nonexudative eye. We further excluded images that had poor quality due to signal strength below 50 or significant motion artifact.

### Optical Coherence Tomography Angiography

Patients underwent imaging with RTVue-XR Avanti device (Optovue Inc., Fremont, CA) with split-spectrum amplitude-decorrelation angiography (SSADA).<sup>22</sup> This device has an A-scan rate of 70,000 scans per second and has a light source of 840 nm and a full-width at half-maximum bandwidth of 45 nm. We obtained  $3 \times 3$ -mm<sup>2</sup> scans centered on the fovea. Two consecutive, cross-sectional B-scans were obtained and each B-scan was comprised of 304 A-scans.

### CNV Determination

To determine presence of a CNV, we viewed OCTA scans of the subclinical CNV eye at the earliest date available. Using AngioVue software (version 2016.1.0.26; Optovue, Inc.), two en face slabs were

created that included both the outer retina and choriocapillaris. The first slab was 90  $\mu\text{m}$  below the inner plexiform (IPL) layer to 50  $\mu\text{m}$  below the RPE and the second slab was 72  $\mu\text{m}$  below the IPL and 34  $\mu\text{m}$  below the RPE. Presence of subclinical CNV was verified by presence on both en face slabs as well as flow signal in corresponding B-scans at a level above Bruch's membrane. Two independent, masked graders independently assessed all images (ADT and AEF).

### Percent Area of Choriocapillaris Nonperfusion Calculation

To calculate the percent area of choriocapillaris nonperfusion (PCAN), we processed  $3 \times 3\text{-mm}^2$  macular scans of eyes with subclinical CNV and their fellow exudative AMD eye using AngioVue software (version 2017.1.0.151; Optovue, Inc.). With the updated software, we were able to manually adjust the segmentation to ensure that en face slabs were in the correct location with respect to their appropriate retinal layer. Images were selected at a time point when there was no or minimal fluid in the exudative eye as to minimize potential shadowing by overlying subretinal hemorrhage or other material. Images from both eyes were taken on the same date and had a quality index greater than 6. To calculate PCAN, we used an algorithm similar to that previously described.<sup>14</sup> In brief, the algorithm relied on thresholding the choriocapillaris to determine areas of nonperfusion. In this study, we relied on the foveal avascular zone to determine the global threshold for nonperfusion. Full thickness retina images were imported into ImageJ software (available at <https://imagej.nih.gov/ij/index.html>; National Institutes of Health, Bethesda, MD) and the threshold was calculated as the mean pixel value in the area within the foveal avascular zone.

We then used the algorithm to further eliminate shadowing in the choriocapillaris due to the overlying superficial capillary plexus (SCP) as well as drusen and CNV. The automated segmentation of the SCP was used to eliminate shadowing of the retinal blood vessels. A 22- $\mu\text{m}$  en face OCT slab at the level of Bruch's membrane was used to eliminate shadowing from drusen, CNV, and thickened RPE (defined as a 50% increase in width from the typical combined width of the RPE and basement membrane). This slab was chosen as it encompassed the typical thickness of the RPE and basement membrane.<sup>23</sup> We manually adjusted and propagated the segment when necessary to ensure the segmentation followed Bruch's mem-

brane. The en face image of the Bruch's membrane slab was then imported into ImageJ and thresholded to eliminate the darkest 30% percentile of pixels to ensure consistent elimination of shadowing regardless of druse or CNV size.

To calculate PCAN, we imported the choriocapillaris slab, SCP and manually segmented Bruch's slabs into the custom MATLAB software (MathWorks, Inc., Natick, MA). After removing all vascular and drusen shadows, the software calculated the percent of pixels in the choriocapillaris below the nonperfusion threshold in the remaining areas. An additional PCAN parameter, called the "halo PCAN," was calculated for the area within 200  $\mu\text{m}$  outside of the CNV border (Fig. 1). Two independent graders determined the global threshold and performed the analysis for PCAN (ADT and PLN).

### Statistical Analysis

We used Statistical Package for Social Sciences (version 21; IBM Corporation, Chicago, IL). To determine the PCAN for each eye, PCAN values were averaged between graders. Intergrader variability was assessed using the intraclass correlation coefficient. A paired samples *t*-test was performed to compare PCAN of the entire choriocapillaris macular slab to the "halo PCAN" for entire CNV population (subclinical and fellow exudative CNV eyes) and to compare PCAN between subclinical CNV and fellow exudative AMD eyes. A *P* value less than 0.05 was considered statistically significant.

## Results

Of the population of 140 patients with AMD imaged on OCTA during our study period, 48 patients were found to have unilateral exudative AMD and nonexudative AMD in the fellow eye. Fourteen patients were excluded due to poor image quality. Of 34 fellow eyes of patients with unilateral exudative AMD included in this study (mean age,  $76.9 \pm 8.6$ ; female 20 [58.8%]), subclinical CNV was detected in five eyes (14.7%; mean age,  $69.8 \pm 8.5$ ; female 2 [40%]; Table 1). Four of the five lesions were type 1 CNVs (located below Bruch's membrane) that were juxtafoveal in location. One lesion was a type 3 CNV (retinal angiomatous proliferation) that was extrafoveal in location (Fig. 2).

All exudative and subclinical CNV eyes had greater halo PCAN as compared with PCAN of the entire  $3 \times 3\text{-mm}^2$  macula scan (Table 2). Combined



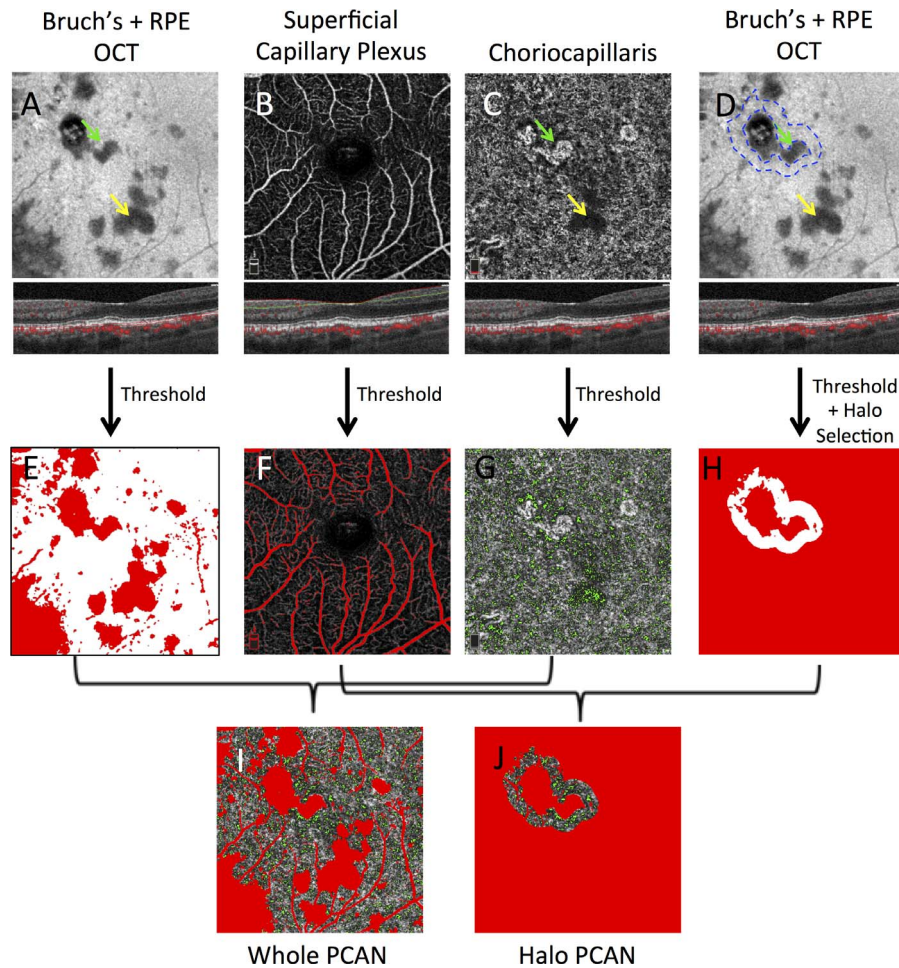


**Figure 1.** Schematic of PCAN for whole  $3 \times 3\text{-mm}^2$  scan of macula and in the  $200\text{-}\mu\text{m}$  halo around CNV. *Green arrows* point to CNV and CNV shadowing. *Yellow arrows* point to druse shadowing. (A,D) OCT slabs of Bruch's membrane and RPE showing shadowing (OCT signal attenuation) from drusen, SCP, and CNV. *Blue lines* outline CNV and area  $200 \mu\text{m}$  outside CNV border (D). (B) OCTA slab of SCP. (C) OCTA slab of choriocapillaris. (E) OCT slab with threshold applied. (F) SCP with threshold applied. (G) Choriocapillaris with PCAN threshold applied. (H) OCT slab with threshold applied and selection of area  $200 \mu\text{m}$  to the outside of the CNV border. (I) *Green pixels* representative of whole PCAN with *red pixels* removed from choriocapillaris area. Comprising image G with overlay of *red pixels* from images E and F. (J) *Green pixels* representative of halo PCAN with *red pixels* removed from choriocapillaris area. Comprising image G with overlay of *red pixels* from images F and H.

CNV mean PCAN and halo PCAN values were  $10.333 \pm 4.288\%$  and  $13.045 \pm 5.809\%$ , respectively ( $P < 0.001$ ).

All subclinical CNV lesions were found in  $3 \times 3\text{-mm}^2$  macular scans and allowed direct comparison of PCAN to  $3 \times 3\text{-mm}^2$  macular scans in the fellow exudative AMD eye. Mean PCAN values for exudative and subclinical CNV eyes were  $11.677 \pm 5.332\%$  and  $8.989 \pm 2.905\%$ , respectively ( $P = 0.138$ ; [Table 2](#)). Mean halo PCAN values for exudative and subclinical CNV eyes were  $15.267 \pm 7.230\%$  and  $10.823 \pm 3.365\%$ , respectively ( $P = 0.115$ ; [Table 2](#)), with a trend for lower PCAN in the subclinical CNV eye as compared with the fellow, exudative eye ([Fig. 3](#)).

**Table 1.** Characteristics of Patients With Subclinical CNV Compared With Remaining Cohort

|                                    | Subclinical CNV Cohort<br>(n = 5) | Remaining Cohort<br>(n = 29) |
|------------------------------------|-----------------------------------|------------------------------|
| Mean age $\pm$ SD                  | 69.8 $\pm$ 8.5                    | 78.1 $\pm$ 8.2               |
| Female (%)                         | 2 (40)                            | 18 (62)                      |
| Mean anti-VEGF Injections $\pm$ SD | 22.4 $\pm$ 13.9                   | 13.7 $\pm$ 23.6              |

SD, standard deviation.

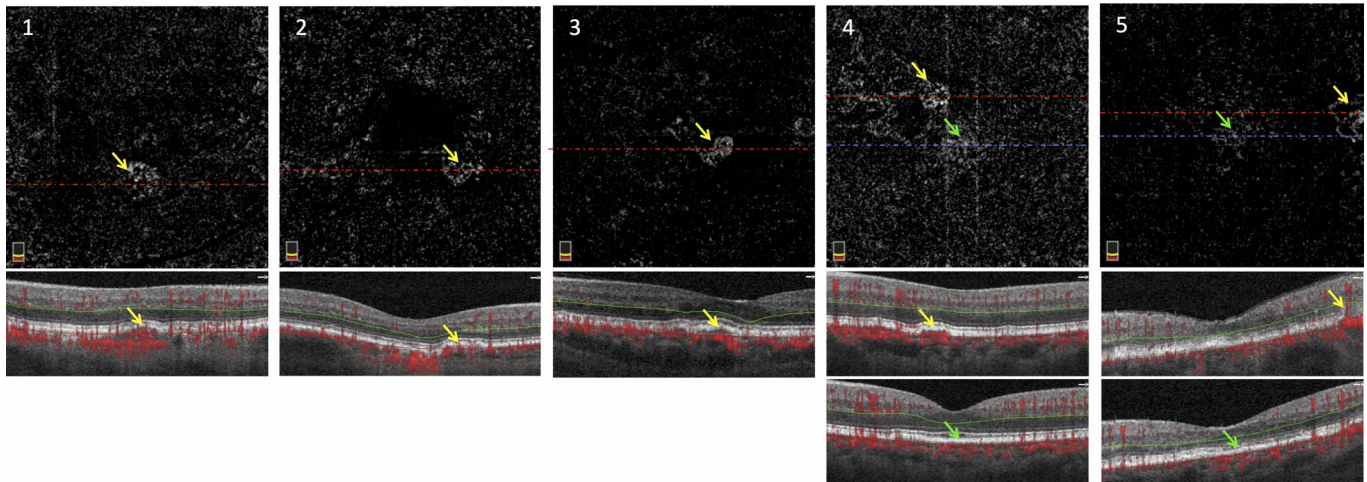


**Figure 2.** OCTA of eyes with subclinical CNV using  $3 \times 3\text{-mm}^2$  scans centered at the fovea. *Yellow arrows* point to CNV lesions. *Green arrows* point to areas of hyperreflectivity on en face scans that do not correspond with CNV lesions. (Top Row) En face slab segmented to include outer retina and superficial choriocapillaris for patients 1 to 5. (Middle Row) Corresponding B-scan through level of CNV lesion. *Yellow arrows* point to flow above Bruch's membrane. CNV lesion is a type 3 for patient 5. All other CNV lesions are type 1 and can be seen below the level of the RPE. (Bottom Row) B-scan through area of hyperreflectivity without corresponding flow. *Green arrows* point to area without flow.

The intraclass correlation coefficient to assess reliability between graders was 0.999 (95% confidence interval [CI] 0.989–1.000) for whole macula PCAN measurements and 0.991 (95% CI 0.959–0.998) for halo PCAN measurements.

Qualitatively, we identified areas of apparent nonperfusion adjacent to CNV lesions on choriocapillaris en face slabs that were not due to loss of choriocapillaris. These areas corresponded with shadowing due to either thickened RPE, CNV lesion, or

subretinal fluid. The corresponding cross-sectional OCT scans confirmed signal attenuation in these areas, which were therefore removed from PCAN calculations (Figs. 4 and 5).

## Discussion

We identified a 15% prevalence of subclinical CNV in fellow eyes of patients with unilateral exudative AMD. In addition, we found significantly increased

**Table 2.** Characteristics of Patients With Unilateral Exudative AMD and Subclinical CNV in Fellow Eye

| Case Number | Age  | Sex | Subclinical CNV Type | Exudative CNV Type | Anti-VEGF Injections (N) | Subclinical CNV Location | Exudative CNV Whole PCAN <sup>a</sup> | Subclinical CNV Whole PCAN <sup>a</sup> | Exudative CNV Halo PCAN <sup>b</sup> | Subclinical CNV Halo PCAN <sup>b</sup> | Combined Whole PCAN <sup>c</sup> | Combined Halo PCAN <sup>c</sup> |
|-------------|------|-----|----------------------|--------------------|--------------------------|--------------------------|---------------------------------------|---|--------------------------------------|--|----------------------------------|---------------------------------|
| 1           | 73   | M   | 1                    | 1                  | 40                       | Juxtafoveal              | 11.730                                | 11.205                                  | 14.835                               | 11.255                                 | 22.935                           | 26.090                          |
| 2           | 74   | F   | 1                    | 1                  | 35                       | Juxtafoveal              | 8.228                                 | 6.531                                   | 12.395                               | 8.326                                  | 14.759                           | 20.721                          |
| 3           | 68   | F   | 1                    | 1                  | 17                       | Juxtafoveal              | 5.510                                 | 6.109                                   | 6.141                                | 8.336                                  | 11.619                           | 14.477                          |
| 4           | 56   | M   | 1                    | 1                  | 1                        | Juxtafoveal              | 19.460                                | 8.354                                   | 25.960                               | 9.758                                  | 27.814                           | 35.718                          |
| 5           | 78   | M   | 3                    | 1                  | 19                       | Extrafoveal              | 13.455                                | 12.745                                  | 17.005                               | 16.440                                 | 26.200                           | 33.445                          |
| Mean        | 69.8 | –   | –                    | –                  | 22.4                     | –                        | 11.677 <sup>d</sup>                   | 8.989 <sup>d</sup>                      | 15.267 <sup>d</sup>                  | 10.823 <sup>d</sup>                    | 10.333 <sup>e</sup>              | 13.045 <sup>e</sup>             |
| P value     | –    | –   | –                    | –                  | –                        | –                        |                                       | 0.138                                   |                                      | 0.115                                  |                                  | <b>0.0007</b>                   |

M, male; F, female; bold indicates statistical significance.

<sup>a</sup> Whole PCAN is the percent choriocapillaris nonperfusion of the entire  $3 \times 3\text{-mm}^2$  macular scan.

<sup>b</sup> Halo PCAN is the percent choriocapillaris nonperfusion of the area within 200  $\mu\text{m}$  of the CNV border.

<sup>c</sup> Combined PCAN is the sum of all exudative and subclinical CNV PCAN values.

<sup>d</sup> Mean is the mean value for all five eyes.

<sup>e</sup> Mean is the mean value for all 10 eyes.



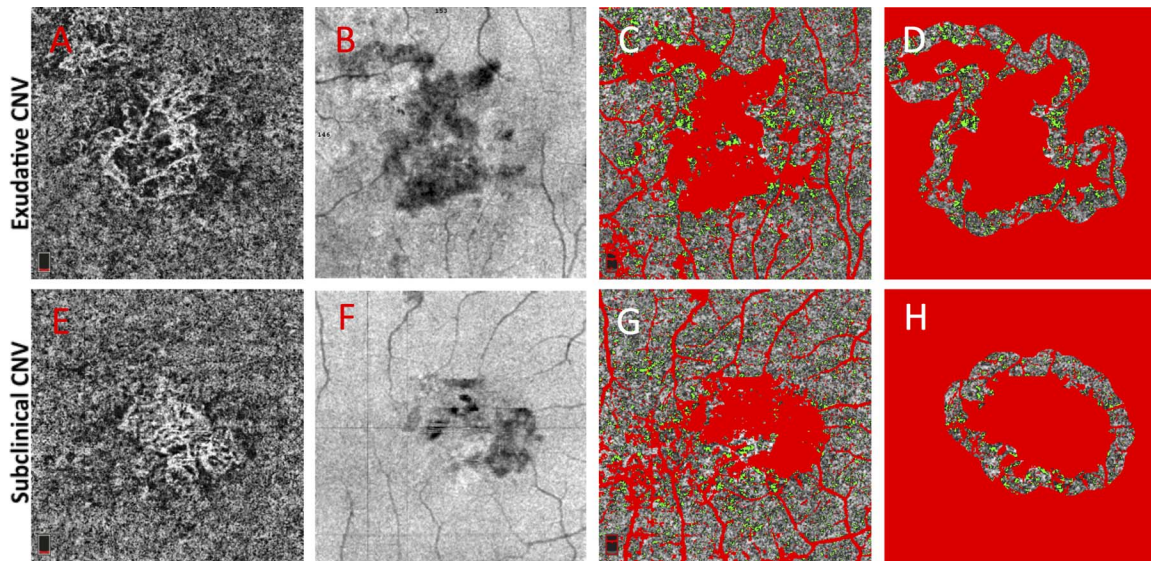


**Figure 3.** OCTA and structural OCT slabs of exudative and subclinical CNV eyes of patient 2 using  $3 \times 3\text{-mm}^2$  scans segmented at the choriocapillaris. (A, E) En face OCTA slabs of exudative (A) and subclinical CNV (E) eyes segmented at choriocapillaris. (B, F) En face OCT slabs of exudative (B) and subclinical (F) CNV eyes segmented to include RPE and Bruch's membrane. Dark areas indicate areas of signal attenuation. (C, G) En face slabs of exudative (C) and subclinical (G) CNV eyes with green area representative of PCAN. Red area indicates shadowing by overlying CNV and SCP and was not included in PCAN calculation. PCAN was 8.228% (C) and 6.531% (G). (D, H) En face slab of exudative (D) and subclinical (H) CNV eyes with green area representative of halo PCAN in an area  $200 \mu\text{m}$  outside of the CNV border. Halo PCAN was 12.395% (D) and 8.326% (H).

choriocapillaris nonperfusion adjacent to CNV lesions as well as a trend for greater choriocapillaris nonperfusion in eyes with exudative AMD as compared to their fellow eyes with subclinical CNV. These results show potentially important applications

for OCTA in quantifying choriocapillaris dysfunction in patients with AMD.

It is important to establish an accurate prevalence of subclinical CNV as these eyes have been shown to have an increased risk of future exudation.<sup>10</sup> OCTA studies have shown a wide range of prevalence of subclinical CNV in fellow eyes of patients with exudative AMD, ranging from 6% to 27% in clinical series at single tertiary care centers.<sup>10–13</sup> Palejwala et al.<sup>12</sup> followed 32 fellow nonexudative AMD eyes of patients with unilateral exudative AMD and determined an initial prevalence of 6% using SD-OCTA. A later, prospective study by Roisman et al.<sup>13</sup> of 11 fellow, intermediate AMD eyes of patients with unilateral exudative AMD found a 27% prevalence of subclinical CNV using swept-source (SS) OCTA. Yanagi et al.<sup>11</sup> used SS-OCTA to prospectively assess 76 fellow eyes of patients with either unilateral exudative AMD or unilateral polypoidal choroidal vasculopathy and determined the prevalence of subclinical CNV to be 18%. Most recently, de Oliveira Dias et al.<sup>10</sup> used SS-OCTA in a prospective study to identify a prevalence of 14% in 160 patients with unilateral exudative AMD. By further stratifying the fellow nonexudative eyes into intermediate AMD and geographic atrophy, the prevalence was determined to be 14% and 16%, respectively.<sup>10</sup>

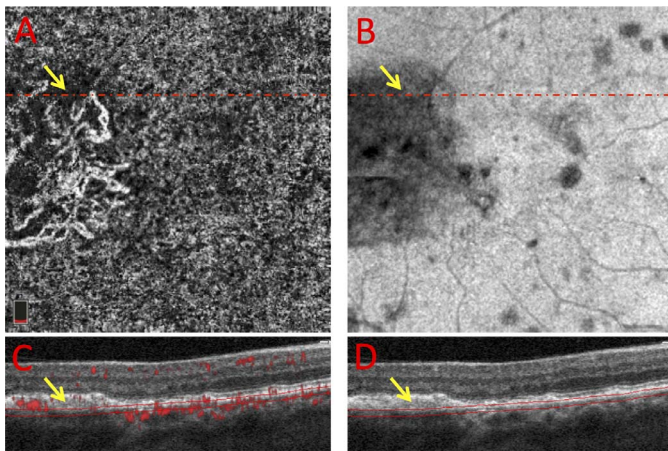


**Figure 4.** OCTA and structural OCT of exudative CNV eye of patient 3 using  $3 \times 3\text{-mm}^2$  macular scans. (A) En face slab shows area that appears to be loss of choriocapillaris adjacent to the CNV lesion. (B) Corresponding OCT confirms that the black area adjacent to the CNV is due to signal attenuation and not loss of choriocapillaris. (C, D) B-scans with (C) and without (D) flow overlay show that there is thick RPE in area of apparent choriocapillaris loss.

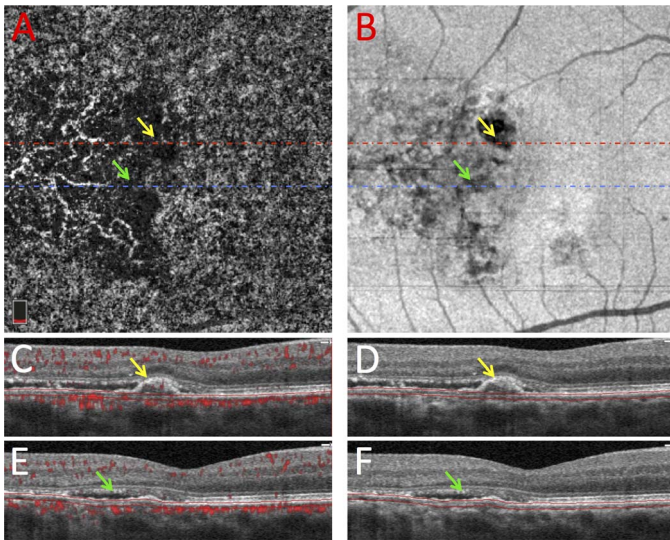


**Figure 5.** OCTA and structural OCT of exudative CNV eye of patient 4 using  $3 \times 3\text{-mm}^2$  macular scans. Arrows point to areas of apparent loss of choriocapillaris. Yellow arrows correspond with top B-scans and green arrows correspond with bottom B-scans. (A) En face slab has areas of apparent choriocapillaris loss adjacent to the CNV lesion. (C, D) B-scans with (C) and without (D) flow overlay show that there is overlying CNV that corresponds with shadowing in the area of apparent choriocapillaris loss. (E, F) B-scans with (E) and without (F) flow overlay show that there is overlying fluid that may correspond with shadowing in area of apparent choriocapillaris loss. (B) Corresponding OCT at level of RPE and Bruch's membrane confirms that black area adjacent to CNV is due to signal attenuation and not loss of choriocapillaris.

The variable prevalence of subclinical CNV in these studies may be explained by a variety of factors, including severity and duration of AMD in the patient cohort. The Comparison of Age Related Macular Degeneration Treatment Trials (CATT) found that fellow eyes of patients treated for unilateral exudative AMD had an increased incidence of CNV development with increasing treatment duration of the exudative eye.<sup>24</sup> In fact, the incidence of CNV in fellow eyes more than doubled when comparing first with second year follow-up.<sup>24</sup> Smaller cohort studies have shown that the incidence of CNV continues to increase beyond 2 years.<sup>3</sup>

OCTA segmentation parameters, projection artifact removal software, and scan density are additional imaging parameters that could potentially affect subclinical CNV detection. The retina and choriocapillaris segmentation protocols were not standardized in these studies and it is likely that algorithms vary in their ability to visualize subclinical CNV lesions. Additionally, some studies relied on en face images and did not verify flow on the corresponding

B-scan. Flow signal in the B-scan has been shown to be crucial, as residual choroidal vessels in atrophy could mimic CNV and potentially confound these studies.<sup>25</sup> Studies further differed in the OCTA scan size used. It is plausible that smaller scans with higher scan density may be better at detecting the earliest subclinical CNV. Alternatively, larger scans, while suffering from lower scan density may capture a wider area and detect more peripheral lesions. Moreover, the imaging wavelength could affect these studies, considering that SS-OCTA uses a longer wavelength, allowing deeper penetration and potentially better detection of these lesions.

The prevalence of subclinical CNV in our study population suggests the importance of heightened vigilance in imaging fellow eyes of patients with unilateral exudative AMD. Larger population studies using OCTA are needed to assess the true prevalence of subclinical CNV, as well as to examine the optimal frequency of imaging required to monitor these fellow eyes for CNV development.

Previous studies have used a variety of modalities to study the association between AMD and choriocapillaris dysfunction. Using ICGA, Ross et al.<sup>19</sup> evaluated early phase hypercyanescent areas and found that eyes with nonexudative and exudative AMD had greater areas of hypoperfusion as compared with healthy controls. Pauleikhoff et al.<sup>20</sup> later found that ICGA hypercyanescent areas in eyes with early AMD corresponded with areas of hypofluorescence on FA. Using laser Doppler flowmetry, Grunwald et al.<sup>21</sup> showed decreased foveolar choriocapillaris flow in AMD eyes with drusen and pigmentary changes as compared with AMD eyes with drusen alone. Choriocapillaris flow was noted to further decrease when the fellow eye had presence of a CNV.<sup>21</sup> Histopathologic analyses have expanded upon these findings by suggesting a primary role of the choriocapillaris in AMD pathogenesis. McLeod et al.<sup>26</sup> studied donor eyes with AMD and found CNV lesions at the borders of RPE and choriocapillaris degeneration. Viable RPE was present in some regions of choriocapillaris degeneration and it was suggested that choriocapillaris loss leads to RPE dysfunction.<sup>26</sup> More recently, Seddon et al.<sup>27</sup> performed a histologic analysis of 32 postmortem eyes with various grades of AMD and found loss of the choriocapillaris without overlying abnormality of the RPE in some eyes with early-stage AMD. Interestingly, in patients with geographic atrophy, RPE atrophy was noted to occur in areas without choriocapillaris loss.<sup>27</sup> These results suggest a poten-



tially different pathogenesis of exudative AMD and geographic atrophy such that choriocapillaris dysfunction may play a more important role in exudative AMD. The pathogenesis of AMD remains multifactorial and complex interactions between genetics, environment, and other host factors, such as smoking, need to be considered.<sup>28</sup> Whether choriocapillaris dysfunction is primary or secondary to accumulation of basal laminar deposits, thickening of Bruch's membrane and impairment of VEGF diffusion remains an area of great debate and study.<sup>29,30</sup>

Recently, OCTA has been used to quantitatively study the choriocapillaris in patients with AMD. These studies showed that eyes with reticular pseudodrusen (RPD) had increased choriocapillaris nonperfusion compared with either AMD eyes without RPD or with healthy controls.<sup>14,31</sup> Interestingly, RPD are also considered a strong risk factor for progression to late AMD,<sup>32</sup> though, in our cohort of patients with subclinical CNV, only one had bilateral RPD, while none had unilateral. Most recently, Borrelli et al.<sup>15</sup> showed that the percent choriocapillaris nonperfusion was not statistically different in intermediate AMD eyes regardless whether the fellow eye had exudative AMD or intermediate AMD. By analyzing the area surrounding the CNV, we found quantitative evidence of choriocapillaris loss in the areas adjacent to exudative and subclinical CNV formation. These results are consistent with previous findings by Jia et al.<sup>33</sup> and Moulton et al.<sup>34</sup> who showed qualitative areas of low decorrelation surrounding CNV lesions on OCTA that could not be attributed to OCT signal attenuation. We suggest the potential utility of frequent OCTA assessment of the choriocapillaris in fellow eyes of patients with nonexudative AMD to identify relative areas of nonperfusion as a possible precursor to CNV formation.

We further found that eyes with exudative AMD tended to have larger areas of choriocapillaris nonperfusion compared with fellow subclinical CNV eyes. This difference in nonperfusion was most notable when comparing halo PCAN measurements between fellow eyes. While our results were not statistically significant, we were limited by a small number of eyes. In addition, one patient in our study had a paradoxical PCAN value that was greater in the subclinical CNV eye as compared with the exudative AMD eye. Upon closer chart review, we found that the subclinical CNV eye had prior evidence of subretinal fluid that resolved without treatment, while the exudative AMD eye had not required anti-VEGF treatment for 17 months. We suspect that these

factors may have partially contributed to the paradoxical PCAN results in this patient.

While the management of subclinical CNV identified on OCTA remains uncertain, there is a dearth of studies that characterize the choriocapillaris in these eyes. We hypothesize that exudation in AMD may be triggered by underlying progression of choriocapillaris nonperfusion such that the resultant RPE hypoxia leads to unleashing of abnormal VEGF signaling with growth and eventual exudations of a CNV. Previous studies have shown that subclinical CNV lesions generally enlarge prior to the time of exudation.<sup>10,35</sup> Future large-scale longitudinal studies will be important to determine whether loss of choriocapillaris is indeed the initial insult in AMD leading to CNV formation and progression to exudation.

Strengths of our study relate to inclusion of patients from a single center with variable duration of exudative disease that is representative of the AMD population at large. In addition, we used a rigorous protocol to detect subclinical CNV, including two masked graders and verification of flow signal above Bruch's membrane. Furthermore, we show excellent reproducibility in our measurements of choriocapillaris nonperfusion. Several limitations to our study exist, including a relatively small number of eyes. Additionally, our study did not visualize the entire CNV lesion in several eyes on the  $3 \times 3\text{-mm}^2$  macula scans. It is possible that choriocapillaris nonperfusion is not uniform around CNV lesions, which could potentially confound our results. Future use of a larger scan size or taking multiple scans to encompass the entire CNV lesion may allow for more accurate PCAN quantification. Our study is further limited by the cross sectional design. While this allowed direct comparison between fellow eyes, we were unable to determine the effects of disease duration or treatment on choriocapillaris nonperfusion. We cannot rule out anti-VEGF therapy as a potential confounder for increased PCAN in exudative AMD eyes. Previous studies have suggested that anti-VEGF therapy may be associated with decreased choroidal thickness in addition to suppressing CNV exudation.<sup>36-38</sup>

In summary, we found a 15% prevalence of subclinical CNV in fellow eyes of patients with unilateral exudative AMD. We also report significantly higher PCAN adjacent to all CNV lesions and a trend of higher PCAN in exudative AMD eyes as compared with their fellow subclinical CNV eyes. These findings suggest the importance of OCTA in quantitatively assessing choriocapillaris dysfunction



in exudative AMD. Incorporation of our quantification methods into commercially available OCTA software may allow for faster analyses, larger scale studies, and validation of current and prior studies. Future longitudinal studies are needed to assess choriocapillaris nonperfusion in subclinical CNV lesions over time, as this could potentially be a useful biomarker that may predict progression to exudation.

## Acknowledgments

Supported by NIH grant DP3-DK108248(AAF) and research instrument support by OptoVue, Inc.

Disclosure: **A.D. Treister**, None; **P.L. Nesper**, None; **A.E. Fayed**, None; **F.K. Gill**, None; **R.G. Mirza**, None; **A.A. Fawzi**, None

## References

- Wong WL, Su X, Li X, et al. Global prevalence of age-related macular degeneration and disease burden projection for 2020 and 2040: a systematic review and meta-analysis. *Lancet Glob Health*. 2014;2:e106–e16.
- Holz FG, Schmitz-Valckenberg S, Fleckenstein M. Recent developments in the treatment of age-related macular degeneration. *J Clin Invest*. 2014;124:1430.
- Maguire MG, Bressler SB, Bressler NM, et al. Risk factors for choroidal neovascularization in the second eye of patients with juxtafoveal or subfoveal choroidal neovascularization secondary to age-related macular degeneration. *Arch Ophthalmol*. 1997;115:741–747.
- Green WR, Key S III. Senile macular degeneration: a histopathologic study. *Trans Am Ophthalmol Soc*. 1977;75:180.
- Sarks S. New vessel formation beneath the retinal pigment epithelium in senile eyes. *Br J Ophthalmol*. 1973;57:951.
- Yannuzzi LA, Slakter JS, Sorenson JA, Guyer DR, Orlock DA. Digital indocyanine green videoangiography and choroidal neovascularization. *Retina*. 1992;12:191–223.
- Hanutsaha P, Guyer DR, Yannuzzi LA, et al. Indocyanine-green videoangiography of drusen as a possible predictive indicator of exudative maculopathy. *Ophthalmology*. 1998;105:1632–1636.
- De Carlo TE, Romano A, Waheed NK, Duker JS. A review of optical coherence tomography angiography (OCTA). *Int J Retina Vitreous*. 2015;1:5.
- Carnevali A, Cicinelli MV, Capuano V, et al. Optical coherence tomography angiography: a useful tool for diagnosis of treatment-naïve quiescent choroidal neovascularization. *Am J Ophthalmol*. 2016;169:189–198.
- de Oliveira Dias JR, Zhang Q, Garcia JM, et al. Natural history of subclinical neovascularization in nonexudative age-related macular degeneration using swept-source OCT angiography. *Ophthalmology*. 2018;125:255–266.
- Yanagi Y, Mohla A, Lee W-K, et al. Prevalence and risk factors for nonexudative neovascularization in fellow eyes of patients with unilateral age-related macular degeneration and polypoidal choroidal vasculopathy. *Invest Ophthalmol Vis Sci*. 2017;58:3488–3495.
- Palejwala NV, Jia Y, Gao SS, et al. Detection of non-exudative choroidal neovascularization in age-related macular degeneration with optical coherence tomography angiography. *Retina*. 2015;35:2204.
- Roisman L, Zhang Q, Wang RK, et al. Optical coherence tomography angiography of asymptomatic neovascularization in intermediate age-related macular degeneration. *Ophthalmology*. 2016;123:1309–1319.
- Nesper PL, Soetikno BT, Fawzi AA. Choriocapillaris nonperfusion is associated with poor visual acuity in eyes with reticular pseudodrusen. *Am J Ophthalmol*. 2017;174:42–55.
- Borrelli E, Uji A, Sarraf D, Sadda SR. Alterations in the choriocapillaris in intermediate age-related macular degeneration. *Invest Ophthalmol Vis Sci*. 2017;58:4792–4798.
- Spaide RF. Choriocapillaris flow features follow a power law distribution: implications for characterization and mechanisms of disease progression. *Am J Ophthalmol*. 2016;170:58–67.
- Ferrara D, Waheed NK, Duker JS. Investigating the choriocapillaris and choroidal vasculature with new optical coherence tomography technologies. *Prog Retin Eye Res*. 2016;52:130–155.
- Ramrattan RS, van der Schaft TL, Mooy CM, De Bruijn W, Mulder P, De Jong P. Morphometric analysis of Bruch's membrane, the choriocapillaris, and the choroid in aging. *Invest Ophthalmol Vis Sci*. 1994;35:2857–2864.
- Ross RD, Barofsky JM, Cohen G, Baber WB, Palao SW, Gitter KA. Presumed macular choroidal watershed vascular filling, choroidal neo-

- vascularization, and systemic vascular disease in patients with age-related macular degeneration. *Am J Ophthalmol*. 1998;125:71–80.
20. Pauleikhoff D, Spital G, Radermacher M, Brumm GA, Lommatzsch A, Bird AC. A fluorescein and indocyanine green angiographic study of choriocapillaris in age-related macular disease. *Arch Ophthalmol*. 1999;117:1353–1358.
  21. Grunwald JE, Metelitsina TI, DuPont JC, Ying G-S, Maguire MG. Reduced foveolar choroidal blood flow in eyes with increasing AMD severity. *Invest Ophthalmol Vis Sci*. 2005;46:1033–1038.
  22. Jia Y, Tan O, Tokayer J, et al. Split-spectrum amplitude-decorrelation angiography with optical coherence tomography. *Opt Express*. 2012;20:4710–4725.
  23. Karampelas M, Sim DA, Keane PA, et al. Evaluation of retinal pigment epithelium–Bruch’s membrane complex thickness in dry age-related macular degeneration using optical coherence tomography. *Br J Ophthalmol*. 2013;97:1256–1261.
  24. Maguire MG, Daniel E, Shah AR, et al. Incidence of choroidal neovascularization in the fellow eye in the comparison of age-related macular degeneration treatments trials. *Ophthalmology*. 2013;120:2035–2041.
  25. Nesper PL, Luttly GA, Fawzi AA. Residual choroidal vessels in atrophy can masquerade as choroidal neovascularization on optical coherence tomography angiography: introducing a clinical and software approach. *Retina*. 2017;38:1289–1300.
  26. McLeod DS, Taomoto M, Otsuji T, Green WR, Sunness JS, Luttly GA. Quantifying changes in RPE and choroidal vasculature in eyes with age-related macular degeneration. *Invest Ophthalmol Vis Sci*. 2002;43:1986–1993.
  27. Seddon JM, McLeod DS, Bhutto IA, et al. Histopathological insights into choroidal vascular loss in clinically documented cases of age-related macular degeneration. *JAMA Ophthalmol*. 2016;134:1272–1280.
  28. Fritsche LG, Igl W, Bailey JNC, et al. A large genome-wide association study of age-related macular degeneration highlights contributions of rare and common variants. *Nat Genet*. 2016;48:134–143.
  29. Mullins RF, Johnson MN, Faidley EA, Skeie JM, Huang J. Choriocapillaris vascular dropout related to density of drusen in human eyes with early age-related macular degeneration. *Invest Ophthalmol Vis Sci*. 2011;52:1606–1612.
  30. Moreira-Neto CA, Moulton EM, Fujimoto JG, Waheed NK, Ferrara D. Choriocapillaris loss in advanced age-related macular degeneration. *J Ophthalmol*. 2018;2018:8125267.
  31. Alten F, Heiduschka P, Clemens CR, Eter N. Exploring choriocapillaris under reticular pseudodrusen using OCT-angiography. *Graefes Arch Clin Exp Ophthalmol*. 2016;254:2165–2173.
  32. Finger RP, Chong E, McGuinness MB, et al. Reticular pseudodrusen and their association with age-related macular degeneration: the Melbourne Collaborative Cohort Study. *Ophthalmology*. 2016;123:599–608.
  33. Jia Y, Bailey ST, Wilson DJ, et al. Quantitative optical coherence tomography angiography of choroidal neovascularization in age-related macular degeneration. *Ophthalmology*. 2014;121:1435–1444.
  34. Moulton E, Choi W, Waheed NK, et al. Ultrahigh-speed swept-source OCT angiography in exudative AMD. *Ophthalmic Surge Lasers Imaging Retina*. 2014;45:496–505.
  35. Querques G, Srour M, Massamba N, et al. Functional characterization and multimodal imaging of treatment-naïve “quiescent” choroidal neovascularization quiescent choroidal neovascularization. *Invest Ophthalmol Vis Sci*. 2013;54:6886–6892.
  36. Koizumi H, Kano M, Yamamoto A, et al. Short-term changes in choroidal thickness after aflibercept therapy for neovascular age-related macular degeneration. *Am J Ophthalmol*. 2015;159:627–633.e1.
  37. Yamazaki T, Koizumi H, Yamagishi T, Kinoshita S. Subfoveal choroidal thickness after ranibizumab therapy for neovascular age-related macular degeneration: 12-month results. *Ophthalmology*. 2012;119:1621–1627.
  38. Julien S, Biesemeier A, Taubitz T, Schraermeyer U. Different effects of intravitreally injected ranibizumab and aflibercept on retinal and choroidal tissues of monkey eyes. *Br J Ophthalmol*. 2014;98:813–825.